Electronic Supplementary Material (ESI) for Journal of Materials Chemistry A.

Hierarchical nanohoneycomb-like $CoMoO_4$-MnO_2 core–shell and Fe_2O_3 nanosheet arrays on 3D graphene foam with excellent supercapacitive performance

Sachin Kumar[1], Ghuzanfar Saeed[1], Nam Hoon Kim[1*] and Joong Hee Lee[1, 2*]

[1]Advanced Materials Institute of BIN Convergence Technology, Dept. of BIN Convergence Technology,Chonbuk National University, Jeonju, Jeonbuk 54896, Republic of Korea

[2]Carbon Composite Research Centre, Department of Polymer Nano Science and Technology, Chonbuk National University, Jeonju, Jeonbuk 54896, Republic of Korea

Supporting Information

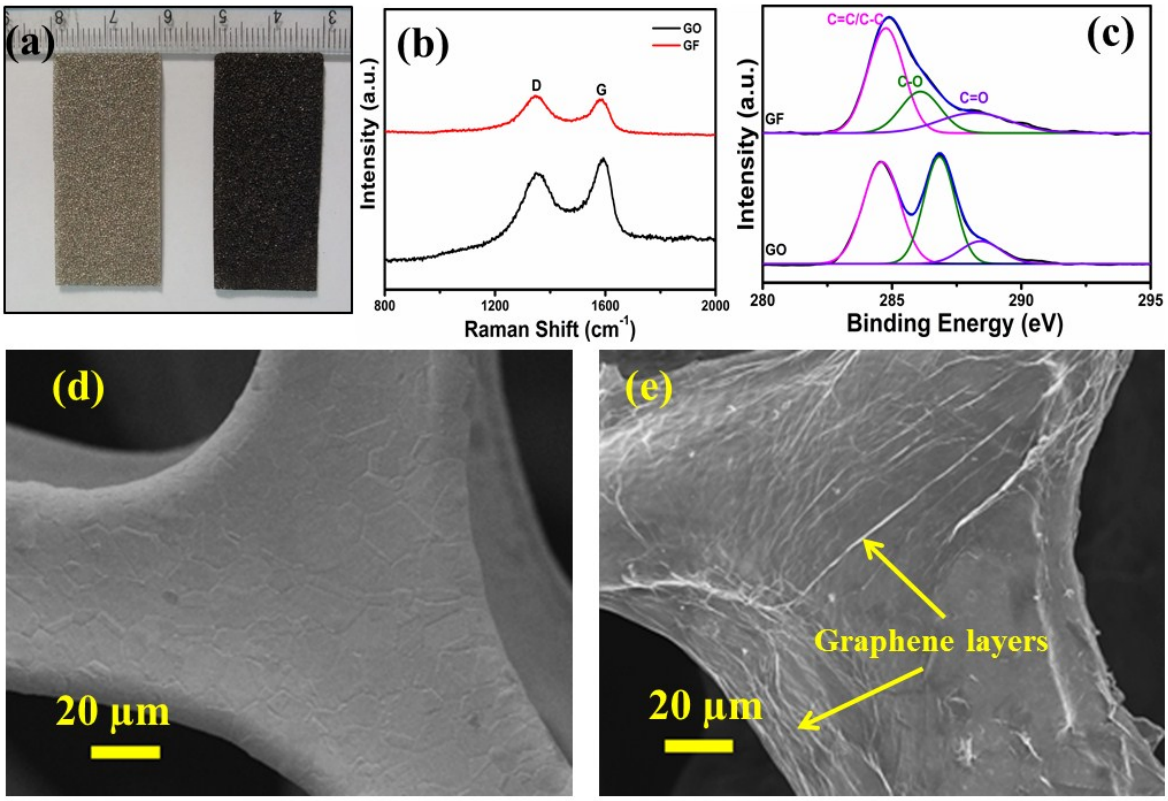

Fig. S1. (a) Optical image of Ni foam (Left) and 3D graphene Foam on Ni foam (Right), (b) Raman spectra of GO and GF, (c) The C 1s spectra of GO and GF (d) FE-SEM images Ni foam and (e) FE-SEM image of 3D graphene foam on Ni scaffold.

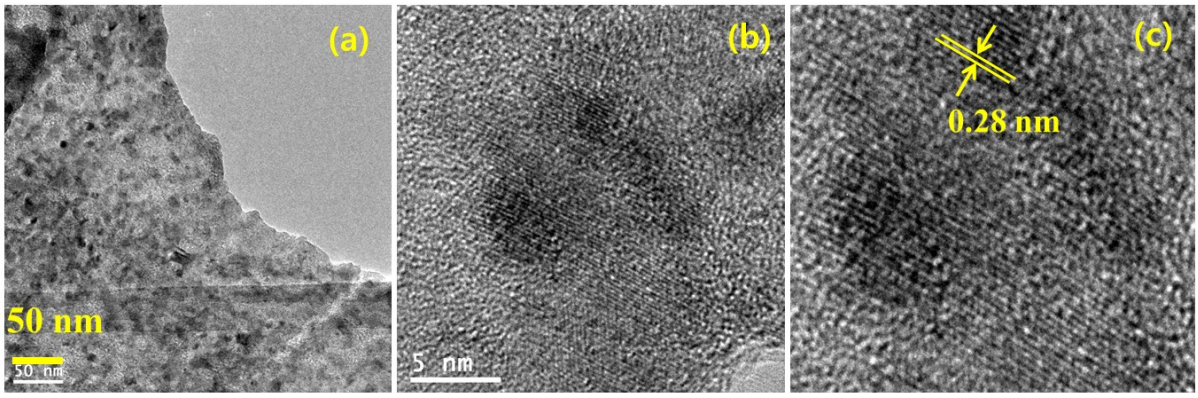

Fig. S2. (a) TEM image of $CoMoO_4$@GF nanosheet arrays (b) HRTEM image and (c) zoomed HRTEM image of $CoMoO_4$@GF.

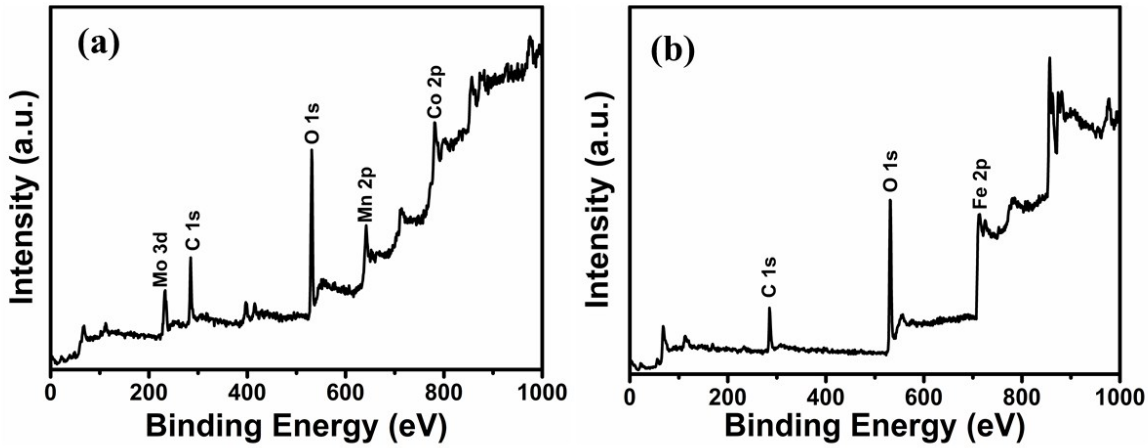

Fig. S3.XPS survey scans of (a) hierarchical nanohoneycomb-like $CoMoO_4$-MnO_2 core-shell and (b) Fe_2O_3 nanosheet arrays, on 3D graphene foam.

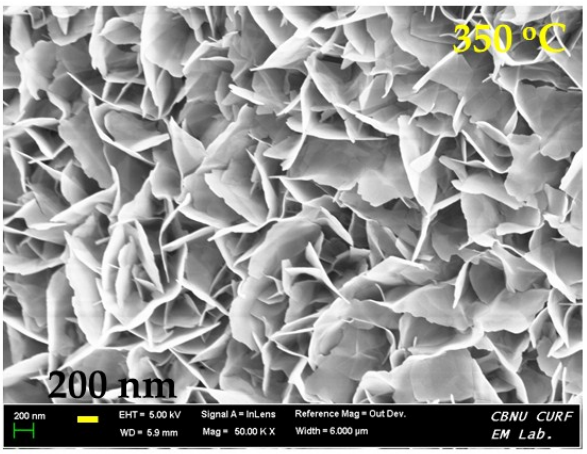

Fig. S4. FE-SEM image of $CoMoO_4$@NF nanosheet arrays annealed at 350 °C.

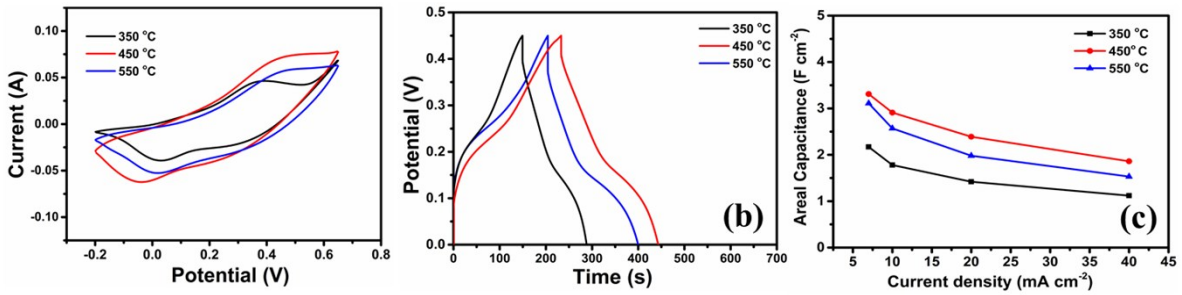

Fig. S5. Comparison of electrochemical properties of $CoMoO_4$@NF nanosheet arrays for different annealing temperature: (a) CV curves at a scan rate of 20 mV s^{-1}, (b) GCD curves at current density of 7 mA cm^{-2} and (c) areal capacitance vs. current density curve for different annealing temperature.

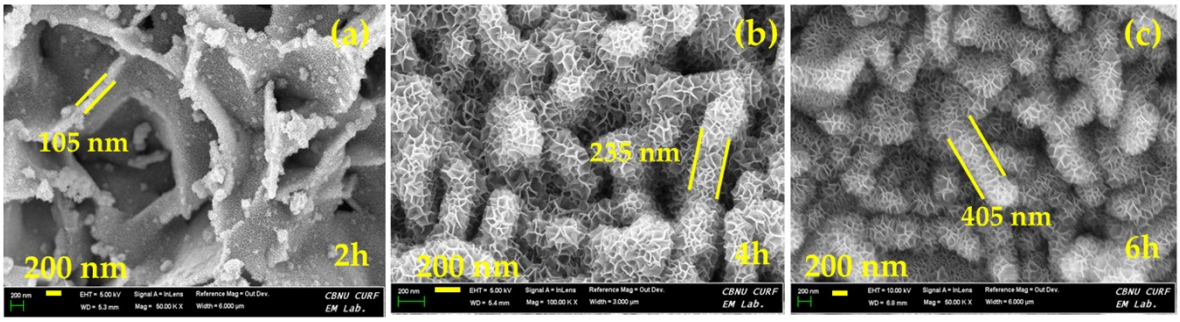

Fig. S6. FE-SEM images of $CoMoO_4$-MnO_2@NF core-shell nanosheet arrays for different reaction time in $KMnO_4$ solution: (a) 2 h (b) 4 h and (c) 6 h.

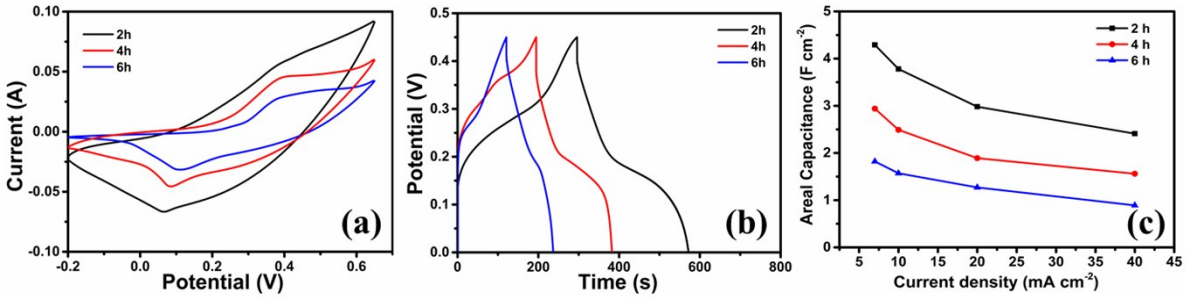

Fig. S7. Comparison of electrochemical properties of $CoMoO_4$-MnO_2@NF core-shell nanosheet arrays for different reaction time in $KMnO_4$ solution: (a) CV curves at a scan rate of 20 mV s^{-1}, (b) GCD curves at current density of 7 mA cm^{-2} and (c) areal capacitance vs. current density curve for different reaction time in $KMnO_4$ solution.

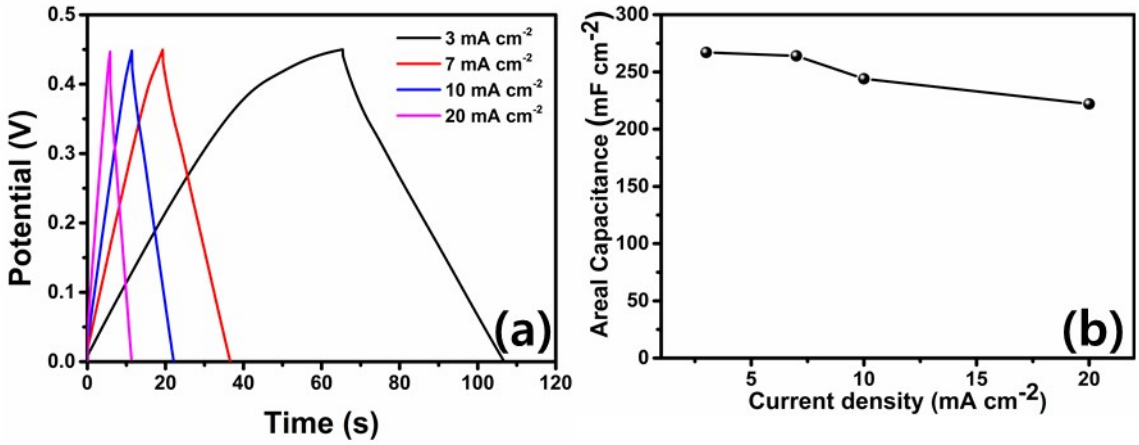

Fig. S8. (a) GCD curve of GF at different current density, (b) areal capacitance measured at different current densities.

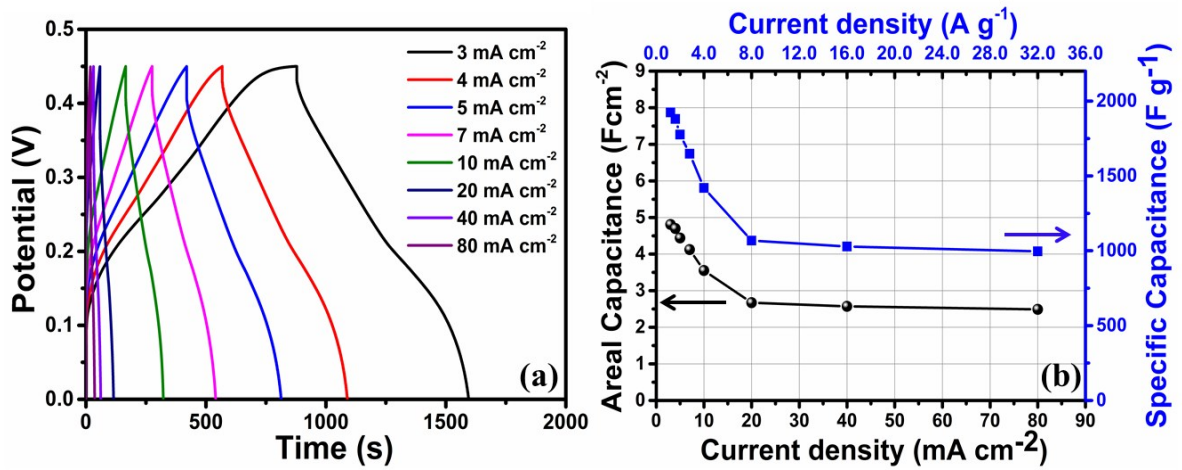

Fig. S9. (a) GCD curve of $CoMoO_4$@GF at different current density, (b) specific and areal capacitance measured at different current densities.

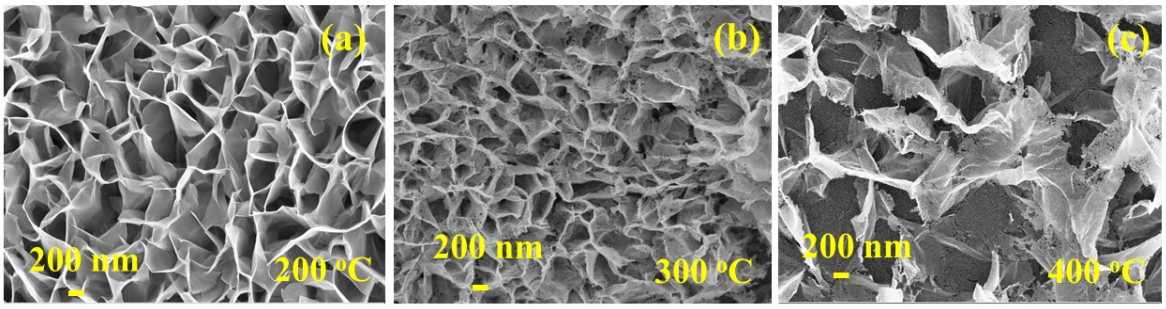

Fig. S10. FE-SEM images of Fe_2O_3@NF nanosheet arrays for different annealing temperatures: (a) 200 (b) 300 and (c) 400 °C.

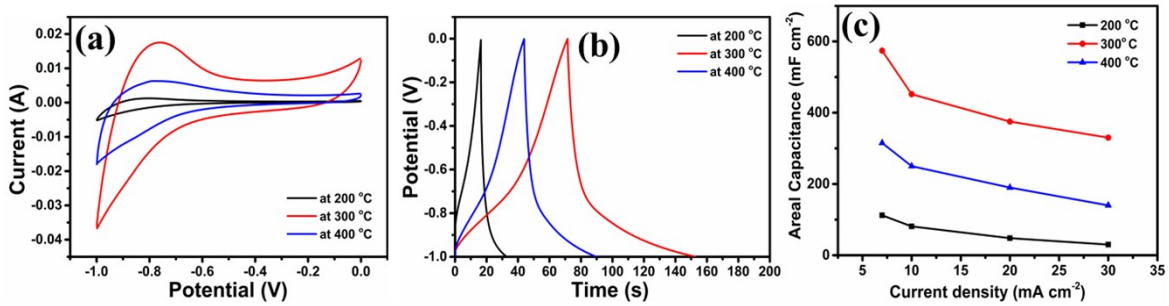

Fig. S11. Comparison of electrochemical properties of Fe_2O_3@NF nanosheet arrays for different annealing temperature: (a) CV curves at a scan rate of 20 mV s^{-1}, (b) GCD curves at current density of 7 mA cm^{-2} and (c) areal capacitance vs. current density curve for different annealing temperature.

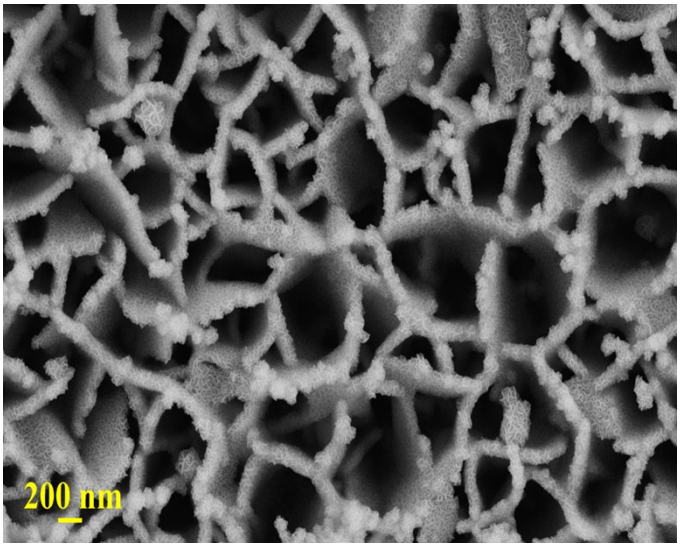

Fig. S12. FE-SEM images of NHC like $CoMoO_4$-MnO_2@GF nanosheet arrays after 10,000 cycles.

Table S1. Comparison of capacitances between the present Fe_2O_3@GF electrode and similar material electrodes taken from the recently published reports.

Electrode materials	Electrolyte	Areal (Specific) capacitance	Current density	Year [Ref.]
α-Fe_2O_3	1 M LiOH	681 mF cm^{-2}	1 mA cm^{-2}	2016 [1]
Fe_2O_3/G	2 M KOH	264 F g^{-1}	2.5 A g^{-1}	2016 [2]
Ti-Fe_2O_3@PEDOT	5 M LiCl	311.6 F g^{-1}	1 mA cm^{-2}	2015 [3]
Fe_2O_3 NDs@NG	2 M KOH	274 F g^{-1}	1 A g^{-1}	2016 [4]
α-Fe_2O_3 nanorods	1 M KOH	500 mF cm^{-2}	2 mA cm^{-2}	2016 [5]
Fe_2O_3/RGO/Fe_3O_4@Fe	2 M KOH	350 mF cm^{-2}	5 mA cm^{-2}	2016 [6]
α-Fe_2O_3/rGO composite	1 M Na_2SO_4	255 F g^{-1}	0.5 A g^{-1}	2017 [7]
Fe_2O_3/PPy@carbon cloth	1 M Na_2SO_4	382.4 mF cm^{-2}	0.5 mA cm^{-2}	2017 [8]
Fe_2O_3@GF nanosheet arrays	**1 M KOH**	**1.26 F cm^{-2} (572.7 F g^{-1})**	**2 mA cm^{-2}**	**This work**

References

[1] X. Zheng, Z. Han, S. Yao, H. Xiao, F. Chai, F. Qu, X. Wu, *Dalton Trans*., 2016, **45**, 7094–7103.

[2] J. Wu, A. Zhou, Z. Huang, L. Li, H. Bai, *Chin. J. Chem.,* 2016, **34**, 67–72.

[3] Y. Zeng, Y. Han, Y. Zhao, Y. Zeng, M. Yu, Y. Liu, H. Tang, Y. Tong, X. Lu, *Adv. Energy mater.,* 2015, **5**, 1402176.

[4] L. Liu, J. Lang, P. Zhang, B. Hu, X. Yan, *ACS Appl. Mater. Interfaces,* 2016, **8**, 9335−9344.

[5] S. Zhang, B. Yin, Z. Wang, F. Peter, *Chem. Eng. J.,* 2016, **306**, 193–203.

[6] C. Zhao, X. Shao, Y. Zhang, X. Qian, *ACS Appl. Mater. Interfaces*, 2016, **8**, 30133−30142.

[7] Y. Zhu, S. Cheng, W. Zhou, J. Jia, L. Yang, M. Yao, M. Wang, J Zhou, P. Wu, M. Liu, *ACS Sustainable Chem. Eng.,* 2017, **5**, 5067−5074.

[8] L. Wang, H. Yang, X. Liu, R. Zeng, M. Li, Y. Huang, X. Hu, *Angew. Chem*., 2017, **129**, 1125 –1130.